NeuroImage: Clinical 11 (2016) 81–89

Contents lists available at ScienceDirect

NeuroImage: Clinical

journal homepage: www.elsevier.com/locate/ynicl

Mean cortical curvature reflects cytoarchitecture restructuring in mild traumatic brain injury

Jace B. King[a,b,c,*], Melissa P. Lopez-Larson[c,d], Deborah A. Yurgelun-Todd[b,c,d,e]

[a]Department of Radiology, University of Utah, 30 North 1900 East #1A071, Salt Lake City, UT 84132-2140, USA
[b]Interdepartmental Program in Neuroscience, University of Utah, 20 South 2030 East, 390A BPRB, Salt Lake City, UT 84112, USA
[c]Diagnostic Neuroimaging, University of Utah, 383 Colorow Drive, Salt Lake City, UT 84108, USA
[d]Department of Psychiatry, University of Utah, 501 Chipeta Way, Salt Lake City, UT 84108, USA
[e]George E. Whalen Department of Veterans Affairs Medical Center, VA VISN 19 Mental Illness Research, Education and Clinical Center (MIRREC), 500 Foothill Drive, Salt Lake City, UT 84148, USA

ARTICLE INFO

Article history:
Received 29 September 2015
Received in revised form 23 November 2015
Accepted 2 January 2016
Available online 6 January 2016

Keywords:
Mean cortical curvature
Mild traumatic brain injury
Cerebral atrophy

ABSTRACT

In the United States alone, the number of persons living with the enduring consequences of traumatic brain injuries is estimated to be between 3.2 and 5 million. This number does not include individuals serving in the United States military or seeking care at Veterans Affairs hospitals. The importance of understanding the neurobiological consequences of mild traumatic brain injury (mTBI) has increased with the return of veterans from conflicts overseas, many of who have suffered this type of brain injury. However, identifying the neuroanatomical regions most affected by mTBI continues to prove challenging. The aim of this study was to assess the use of mean cortical curvature as a potential indicator of progressive tissue loss in a cross-sectional sample of 54 veterans with mTBI compared to 31 controls evaluated with MRI. It was hypothesized that mean cortical curvature would be increased in veterans with mTBI, relative to controls, due in part to cortical restructuring related to tissue volume loss. Mean cortical curvature was assessed in 60 bilateral regions (31 sulcal, 29 gyral). Of the 120 regions investigated, nearly 50% demonstrated significantly increased mean cortical curvature in mTBI relative to controls with 25% remaining significant following multiple comparison correction (all, pFDR < .05). These differences were most prominent in deep gray matter regions of the cortex. Additionally, significant relationships were found between mean cortical curvature and gray and white matter volumes (all, $p < .05$). These findings suggest potentially unique patterns of atrophy by region and indicate that changes in brain microstructure due to mTBI are sensitive to measures of mean curvature.

1. Introduction

The number of persons living with the enduring consequences of traumatic brain injuries (TBI) is estimated to be between 3.2 and 5 million people in the United States alone (Coronado et al., 2012). In 2010, the Centers for Disease Control and Prevention estimated that 2.5 million emergency department visits were TBI related (Centers for Disease Control and Prevention, 2014). However, individuals serving in the United States military or seeking care at Veterans Affairs hospitals are not accounted for in those estimates suggesting the true incidence of TBI is widely underestimated (Centers for Disease Control and Prevention, 2014). With the recent return of veterans from conflicts overseas, increasing pressure is being placed on the medical community to better understand the neurobiological consequences of mild traumatic brain injury (mTBI). However, identifying the regions of the brain most affected by mTBI continues to prove challenging due primarily to the heterogeneous nature of these injuries (Irimia et al., 2014) and diagnostic complexities (Buck, 2011; Shenton et al., 2012; Amyot et al., 2015). Cortical contusions, which involve gray matter and contiguous subcortical white matter, and diffuse axonal injury are two of the most common types of nonpenetrating TBI, which often result in focal damage to the inferior, lateral and anterior aspects of the frontal and temporal lobes and at the gray–white matter junction respectively (Osborn, 2010). Additionally, rapid acceleration or deceleration can lead to focal shear injuries, which are caused by rotational forces, shear, and/or strain on the axon typically at the gray–white matter junction (Bigler, 2001). It has also been suggested that sulcal regions may be biomechanically vulnerable to the dynamic forces associated with the injury which may explain why neurofibrillary tangles are often associated with sulci in chronic traumatic encephalopathy (Smith et al., 2013). Furthermore, recent evidence suggests that tissue pathology related to TBI can be progressive and chronic (Ding et al., 2008; Cole et al., 2015).

* Corresponding author at: University of Utah, Imaging and Neurosciences Center, 729 Arapeen Drive, Salt Lake City, UT 84108, USA.
E-mail addresses: jace.king@hsc.utah.edu (J.B. King), melissa.lopez-larson@hsc.utah.edu (M.P. Lopez-Larson), deborah.yurgelun-todd@hsc.utah.edu (D.A. Yurgelun-Todd).

http://dx.doi.org/10.1016/j.nicl.2016.01.003

Numerous neuroimaging techniques have been used to investigate changes to brain integrity related to TBI including structural magnetic resonance imaging (MRI), functional MRI (fMRI), diffusion tensor imaging (DTI), magnetoencephalography, positron emission tomography, and macromolecular proton fraction (Huang et al., 2009; Bigler et al., 2010; Yurgelun-Todd et al., 2011; Lopez-Larson et al., 2013; Han et al., 2014; Petrie et al., 2014). Despite the many limitations inherent in studying TBI, progress has been made as emerging technologies allow for novel uses of neuroimaging data to study the effects of TBI. For example, Palacios et al. (2013) examined the contrast between gray and white matter signal intensities between 26 subjects with traumatic axonal injury and 22 controls. They found a pattern of white matter/gray matter contrast reduction in widespread regions of the brain in the TBI group relative to controls. Functional connectivity, a measure of voxel to voxel synchrony based on BOLD fMRI signal, is more frequently being applied to investigate the neuropathology associated with mTBI. Recent advances with this approach are highlighted in Mayer et al. (2015) in a review of the current state of research related to fMRI findings in mTBI populations. In one recent example, Iraji et al. (2015) measured functional connectivity in 358 dense individualized common connectivity based cortical landmarks in 16 mTBI patients compared to 24 controls and found regions of functional hyperconnectivity in the mTBI group. The authors suggest that mTBI may result in connectome-scale brain network connectivity changes resulting in hyper-activation to compensate for the physiological disturbance. Maudsley et al. (2015) used magnetic resonance diffusion and spectroscopy measures to investigate altered metabolism and axonal injury in 40 subjects with a range of TBI severities compared to controls. They found widespread alteration of tissue metabolites in the TBI group relative to controls characterized primarily by increased choline in the cerebellum and cerebrum. A between-group voxel-based analysis using DTI measures revealed few regions with altered fractional anisotropy or mean diffusivity in the TBI group compared to controls. In another example, Trivedi et al. (2007) used SIENA, a package included in the FSL imaging suite, to investigate longitudinal changes to global brain volumes in 37 patients with mild to severe TBI scanned on average of 79 and 409 days post-injury. Longitudinal data from the TBI group were also compared to a control group scanned approximately 6 months apart. Significantly greater percent brain volume change was reported in the TBI group relative to controls. Greater percent brain volume changes were also associated with a longer post-injury coma durations suggesting a relationship between TBI severity and cerebral atrophy. Despite the wide range of TBI severities, many recent neuroimaging studies have begun to focus on mTBI as it is one of the most common types of head injury as well as one of the most difficult to diagnose (Amyot et al., 2015).

As the technology and methods associated with MR acquisition and processing advance, so does the ability to detect finer microstructural alterations to the cortex. Recent advances in the reconstruction of the cortex allow for separate calculation of mean cortical curvature in brain's gyri and sulci. Curvature provides a function of how a point on the surface of the cortex is embedded in space. Mean cortical curvature is made up of the average of principal curvatures derived from the inverse of the radius of the osculating circles at each point on the surface on the gray–white matter junction. Thus, mean cortical curvature values provide a quantitative illustration of the folding of the cortex with convex areas indicating gyral regions and concave areas designating sulcal regions. Increased mean curvature denotes areas with sharper cortical folds than regions with decreased mean curvature. As such, increased cortical curvature in gyri leads to a more “pointed” or “peaked” appearance while increased cortical curvature in sulci indicates a sharper downward trajectory.

It has been suggested that increased cortical curvature may be a biomarker for white matter atrophy (Deppe et al., 2014). Furthermore, cortical curvature has been used to investigate sex differences in gyrification (Luders et al., 2006) and changes to cortical morphology as part of normal cortical development and aging (Pienaar et al., 2008; Operto et al., 2012; Wang et al., 2014). Cortical curvature has also been measured to study cortical malformations and/or atrophy related to developmental (Schaer et al., 2008), neurodegenerative (Im et al., 2008), neurological (Ronan et al., 2011; Deppe et al., 2014), and psychiatric disorders (Ronan et al., 2012).

The aim of the current study was to evaluate the use of extrinsic mean cortical curvature as a potential indicator of progressive tissue loss in a cross-sectional sample of veterans with mTBI as compared to controls. It was hypothesized that mean cortical curvature would be increased in veterans with mTBI, relative to controls, due in part to cortical restructuring related to tissue volume loss and that this increase in curvature would be more robust in deeper regions (sulci) of the cortex as opposed to more superficial regions (gyri). Furthermore, it was predicted that increases in mean cortical curvature would be associated with irregularities in both gray and white matter volumes.

2. Methods and materials

2.1. Subjects

The Institutional Review Boards at the University of Utah and the George E. Whalen Department of Veterans Affairs (VA) Medical Center approved this study. All subjects provided written informed consent prior to study participation. A total of 62 males with mTBI and 40 male controls were recruited from the George E. Whalen VA Medical Center and the community via local advertisements and by word of mouth. Inclusion criteria for all participants in this analysis were: ages 18–55 years old. The Ohio State University-TBI Identification Method (OSU-TBI) was used to determine presence, number, and severity of lifetime TBI injuries (Corrigan and Bogner, 2007). Participants were considered to have a mTBI if they reported an injury event to the head followed by an alteration or loss of consciousness (LOC) (Belanger et al., 2009). Mild brain injury events were defined as a LOC for 30 min or less. Only participants with mTBI that occurred after the age of 12 were considered for inclusion in this study.

Control comparison participants were required to be free from having a current major DSM-IV Axis I diagnosis based on clinical interviews. Exclusion criteria for all subjects included major sensorimotor handicaps (e.g., deafness, blindness, paralysis), estimated full scale IQ < 80, history of claustrophobia, autism, schizophrenia, anorexia nervosa or bulimia, active medical or neurological disease other than mTBI that would impact neurobiology or brain function, history of electroconvulsive therapy; and metal fragments or implants that would be contraindicated in an MRI.

All participants, including controls, completed the Structured Clinical Interview for DSM-IV Patient Version (SCID-I/P) (First et al., 1996) administered by trained clinicians. Diagnoses of mTBI and any DSM-IV diagnosis/diagnoses were confirmed via clinician consensus. The DSM-IV-TR Global Assessment of Functioning (GAF) (American Psychiatric Association, 2000) was used to subjectively rate occupational, social, and psychological functioning on a scale of 1 (worst) to 100 (best).

2.2. Data acquisition and processing

2.2.1. MRI data acquisition

Acquisition of imaging data was performed at the Utah Center for Advanced Imaging Research (UCAIR) using a 3.0-T Siemens Trio scanner. Structural data was acquired using a T1-weighted 3D MPRAGE GRAPPA sequence acquired sagittally using a 12-channel head coil with TE/TR/TI = 3.38 ms/2.0 s/1.1 s, 8° flip, 256 × 256 acquisition matrix, 256 mm^2 FOV, 160 slices, 1.0 mm slice thickness. Original images were transferred from the scanner in DICOM format and coded. Participants' MRI scans were reviewed by a board-certified CAQ neuroradiologist to rule out gross pathology.

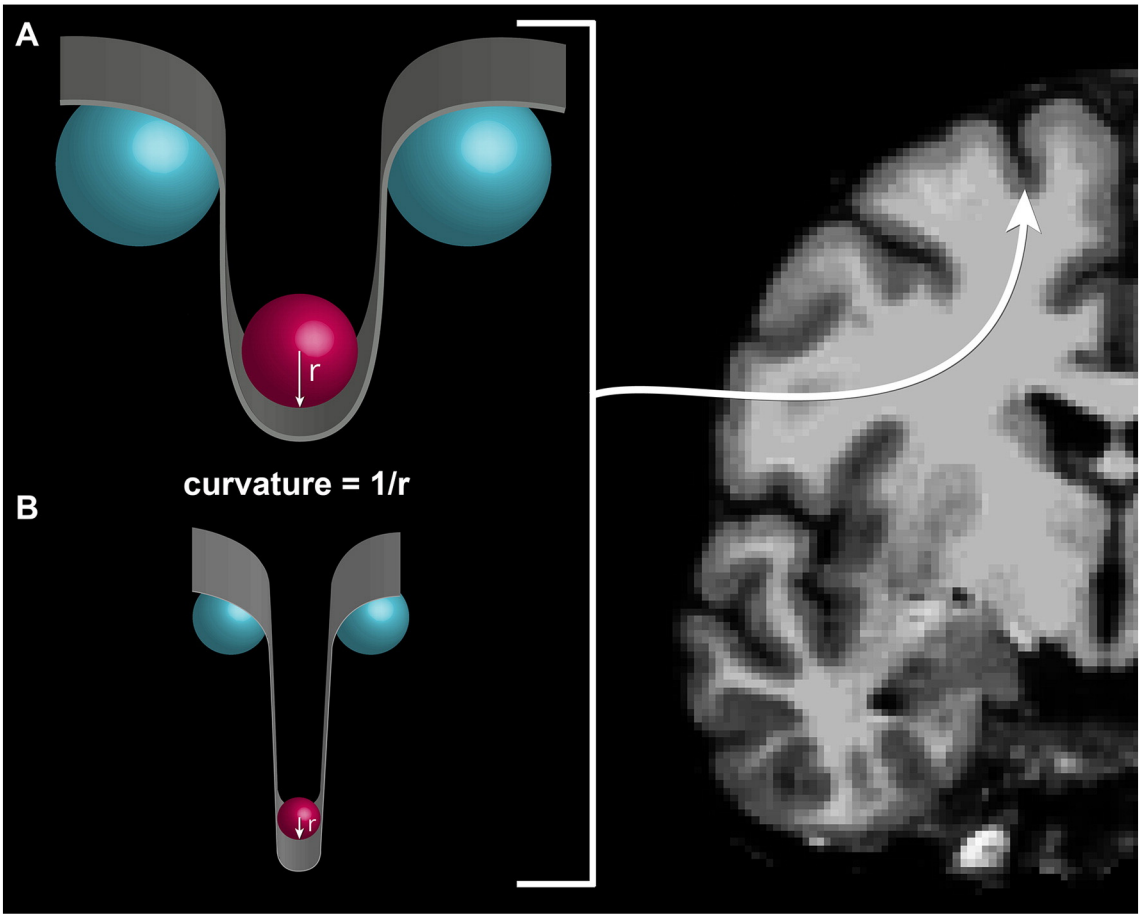

Fig. 1. Example of mean cortical curvature as appears in instances of A) decreasing cortical curvature and B) increasing cortical curvature.

2.2.2. MRI data processing

The FreeSurfer imaging analysis environment (v5.3.0), which is documented and freely available for download (http://surfer.nmr.mgh.harvard.edu/), was used to assess the integrated rectified mean curvature of the cortex and as well as brain volumes. A detailed description of the morphometric procedures used in the FreeSurfer pipeline can be found on the FreeSurfer website. Briefly, images were motion corrected, followed by the removal of non-brain tissue using a hybrid watershed/surface deformation procedure (Segonne et al., 2004), automated transformation to Talairach space, deep gray matter and

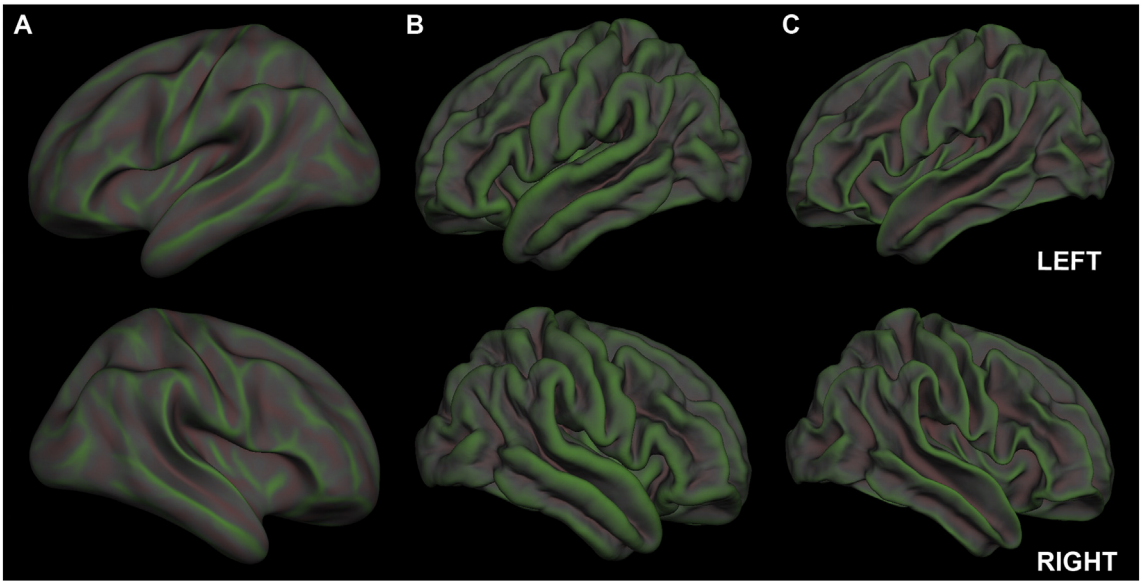

Fig. 2. Rendition of mean cortical curvature as it appears on an inflated surface (A), the pial surface (B), and the white matter surface (C). Curvature in sulcal regions is displayed in green while curvature in gyral regions is displayed in red. (For interpretation of the references to color in this figure legend, the reader is referred to the web version of this article.)

subcortical white matter segmentations (Fischl et al., 2002, 2004a), intensity normalization (Sled et al., 1998), tessellation of the white and gray matter boundary, automated topology correction (Fischl et al., 2001; Segonne et al., 2007), and surface deformation following intensity gradients leading to border placement of gray/cerebrospinal fluid and gray/white at the location where there is the greatest intensity shift thereby defining tissue class transition (Dale and Sereno, 1993; Dale et al., 1999; Fischl and Dale, 2000). Quality control was performed by a trained operator (JBK) throughout MRI processing within the FreeSurfer environment via manual visual inspection of the output for each subject to ensure proper integrity. No subjects included in this study required any manual edits to surface topology.

2.2.3. MRI data segmentation

Mean cortical curvature is made up of the average of principal curvatures derived from the inverse of the radius of the osculating circles at each point on the surface on the gray–white matter junction (see Figs. 1 and 2). Mean cortical curvature values were derived from the Destrieux cortical atlas (Destrieux et al., 2010). The Destrieux atlas includes cortical parcellation data constructed by first segmenting the cortex into gyral and sulcal regions based on average convexity and then mean curvature of the surface. Additionally, a Bayesian maximum a posteriori model was used to integrate observed surface geometry and the atlas function. The cortex is then further divided into 74 structures in each hemisphere using a manually parcellated healthy human brain template (Fischl et al., 2004b). Only parcellations that were distinctly sulcal or gyral were considered for inclusion in this study resulting in 60 bilateral regions (31 sulcal, 29 gyral). Subcortical parcellation volumetric data, including cerebral white matter and gray volumes, were derived from a technique involving multiple local feature-based statistical classifications that account for individual anatomical variability (Fischl et al., 2002). Lobular gray matter volumes were also extracted for analysis where frontal, parietal, temporal, occipital, cingulate, and insular lobes were based on the Desikan–Killiany atlas (Desikan et al., 2006). Mean cortical curvature values for each lobe were also evaluated.

2.3. Statistical analyses

Statistical analyses were completed using SPSS software (version 23) for Mac OS X. Subject data were normalized in order to meet assumptions for statistical analyses by converting mean cortical curvature data for all 120 regions into z-scores and then removing subjects with values greater than or equal to an absolute value of 3.5 (Guadalupe et al., 2015). Two-sample t-tests were used to compare age and clinical differences between groups. Total white, gray, and lobular gray matter volumes were adjusted for whole brain volume in order to account for individual volumetric differences and then compared between groups using univariate analyses while controlling for age. As this study's a priori hypothesis predicted the directionality of mean cortical curvature group differences, one-tailed values were used for regional and lobular mean cortical curvature group comparisons. Correction for multiple comparisons was performed on the 120 regional analyses using Benjamini and Hochberg's method for false discovery rate (FDR) detection (Benjamini and Hochberg, 1995) in MATLAB (version MATLAB_R2015a; MathWorks, Natick, MA).

To examine the possible relationship between mean cortical curvature and brain volumes, *post hoc* Pearson correlation coefficients were performed with whole brain adjusted white and gray matter volumes in each hemisphere for regions indicating significant differences in the mean curvature analysis in the mTBI group. Given the recruitment strategy employed in the current study, clinical characteristics at time of injury or immediately post-injury were not available. Furthermore, individuals with mTBI often report few if any symptoms, thus measures such as the Glasgow Severity Scale do not capture the sequelae of the injury. In the current study, incident related variables, including age at first injury and time elapsed since injury, were evaluated for potential associations with mean cortical curvature and volumes using Pearson's correlation coefficients. Finally, *post hoc* univariate analyses were used to test for effects of age on between group analyses of mean cortical curvature.

Table 1
Demographic and select subject variables.

	mTBI (N = 54)		Controls (N = 31)		*p*-Value
	Mean	Std.	Mean	Std.	
Age	35.56	8.32	33.77	10.23	ns
GAF	62.41	12.98	83.14	9.12	<.001
Age at first injury after the age of 12 (years)	20.70	6.19	–	–	–
Time since most recent TBI (months)	103.28	92.58	–	–	–

3. Results

3.1. Demographics comparison between mTBI and control groups

Fifty-four veterans with mTBI and 31 controls subjects remained following data normalization, which consisted of removing subjects with mean curvature z-scores greater than or equal to an absolute value of 3.5 (Guadalupe et al., 2015). Age distributions were similar between diagnostic groups (see Table 1). The mTBI group had significantly lower GAF scores compared to controls. Of the veteran mTBI sample, 40 had a current or past history of a psychiatric disorder.

Table 2
Between-group differences comparing mean cortical curvature.

Region	mTBI (N = 54)		Control (N = 31)		*p*FDR
	Mean	Std.	Mean	Std.	
Left hemisphere					
Gyri					
Anterior transverse temporal (Heschl)	.148	.016	.137	.015	.027
Middle occipital	.157	.009	.152	.007	.027
Superior frontal	.161	.009	.155	.008	.027
Angular	.156	.008	.151	.007	.030
Medial occipito-temporal (lingual)	.175	.009	.170	.010	.030
Inferior frontal (opercular)	.154	.010	.149	.006	.037
Supramarginal	.156	.008	.151	.006	.041
Precentral	.150	.017	.142	.011	.048
Sulci					
Intraparietal sulcus & transverse parietal	.126	.008	.121	.007	.027
Suborbital	.148	.018	.136	.016	.027
Inferior temporal	.131	.008	.125	.010	.030
Medial orbital	.150	.009	.144	.008	.030
Parieto-occipital	.134	.009	.129	.007	.030
Superior & transverse occipital	.134	.011	.127	.011	.030
Superior segment of the circular insula	.118	.007	.114	.007	.048
Right hemisphere					
Gyri					
Lateral occipito-temporal (fusiform)	.166	.011	.159	.009	.027
Superior frontal	.164	.010	.157	.006	.027
Superior parietal lobule	.146	.010	.140	.008	.027
Middle temporal	.167	.012	.160	.011	.040
Sulci					
Superior frontal	.127	.008	.121	.008	.027
Inferior frontal	.135	.007	.130	.009	.030
Inferior part of the precentral	.126	.008	.122	.008	.030
Parieto-occipital	.138	.010	.132	.007	.030
Suborbital	.146	.018	.135	.021	.030
Superior & transverse occipital	.140	.011	.133	.008	.030
Superior segment of the circular insula	.122	.008	.118	.006	.030
Superior temporal	.125	.007	.121	.006	.030
Intermedius primus (of Jensen)	.129	.012	.122	.011	.037
Medial occipito-temporal (lingual)	.125	.008	.120	.008	.037
Middle occipital and lunatus	.142	.011	.136	.010	.037

3.2. Between-group morphometric analyses results

Of the 120 regions investigated, the mTBI group demonstrated increased mean cortical curvature in 115 regions relative to controls. Prior to multiple comparison correction, 58 of the 120 regions were significantly increased in mTBI compared to controls with 30 of those regions surviving FDR correction (all, pFDR < .05). Put another way, nearly 50% of the regions investigated demonstrated significantly increased mean cortical curvature in mTBI relative to controls with 25% remaining significant following multiple comparison correction. The 30 regions surviving multiple comparison correction were equally split between hemispheres with 12 in gyral regions and 18 in sulcal regions (see Table 2 and Fig. 3). Four regions were found to have significantly increased mean cortical curvature in the mTBI group bilaterally. No regions indicated significantly increased mean curvature in the control group relative to mTBI. The right cingulate marginalis turned out to be significant (pFDR = .036) when controlling for age while the left precentral gyrus and the left superior part of the circular insular sulcus were no longer significant. Extracting an average mean cortical curvature value for each of the six lobes in both the left and right hemisphere revealed a significant increase in mean cortical curvature in the bilateral frontal ($p \leq .001$), parietal ($p \leq .01$), temporal ($p \leq .01$), occipital ($p \leq .01$), and cingulate ($p < .05$) lobes as well as the right insular lobe ($p = .017$). All lobular mean curvature analyses remained significant when controlling for effects of age. Total brain volumes were reduced in mTBI compared to controls, however not significantly. Additionally, no significant between group differences were found for left, right, or total gray or white matter volumes. When comparing lobular gray matter volumes between groups, no significant differences were found between left and right frontal, parietal, temporal, occipital, cingulate, and insular lobes.

3.3. Correlations between mean cortical curvature and brain volumes

Nine of the 30 identified regions demonstrating significantly increased mean cortical curvature in mTBI compared to controls were found to significantly correlate with white matter volumes (1 gyral, 8 sulcal) (see Table 3 and Fig. 4). Six regions were found to significantly correlate with gray matter volumes (1 gyral, 5 sulcal). Four sulcal regions were significantly correlated with both white and gray matter volumes. Interestingly, correlations with white matter in gyral regions were negative while correlations with sulcal regions were positive. Conversely, correlations with gray matter in gyral regions were positive while the sulcal region demonstrated a negative correlation.

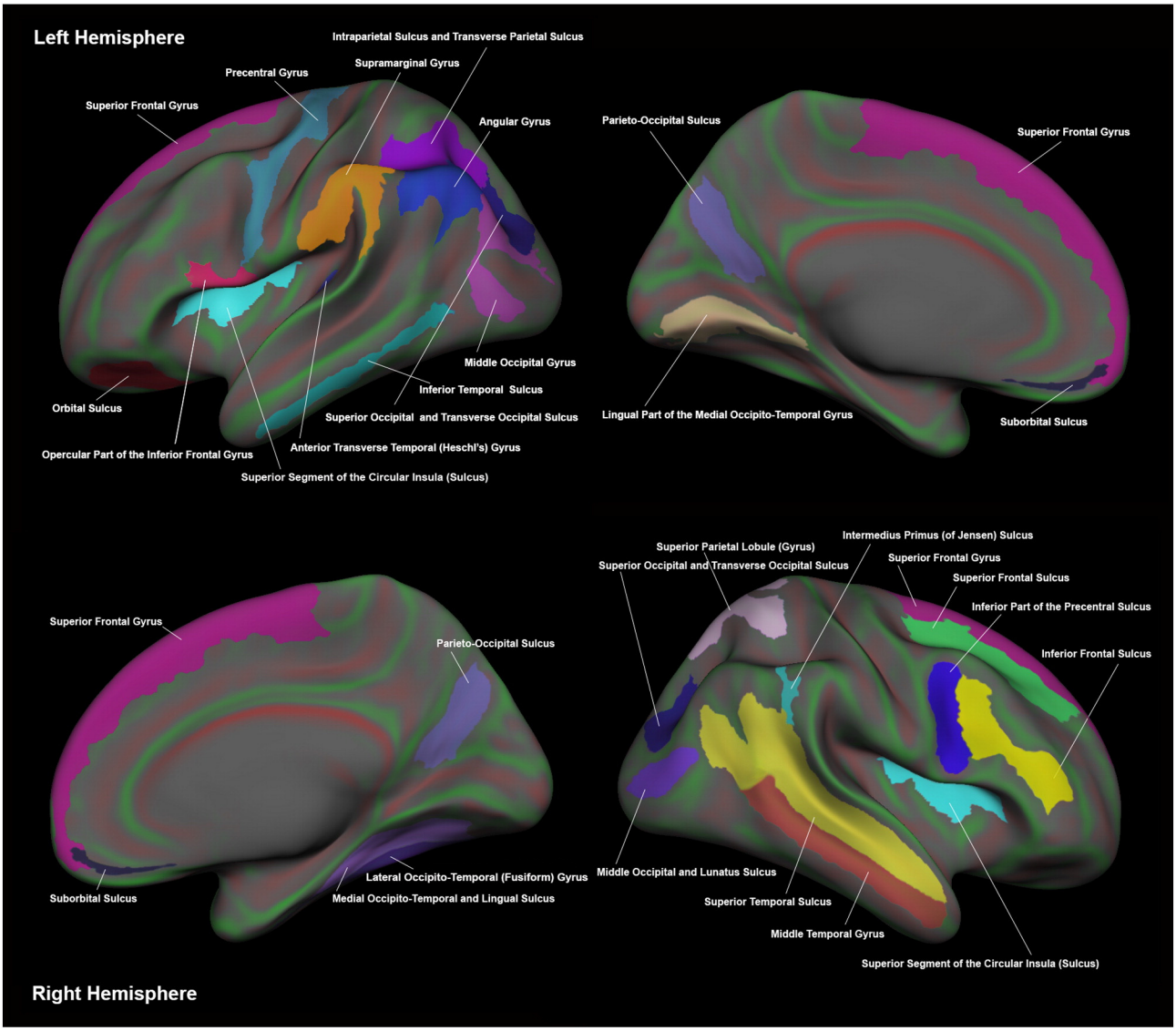

Fig. 3. Representation of regions demonstrating increased mean cortical curvature in mTBI compared to controls.

Table 3
Correlations in the mTBI group between mean cortical curvature and adjusted white and gray matter volumes.

	White		Gray	
	r	*p*	*r*	*p*
Left hemisphere				
Inferior frontal gyrus (opercular)	−.274	.011	ns	ns
Superior segment of the circular insular sulcus	.452	<.001	−.222	.041
Superior & transverse occipital sulcus	.234	.031	−.262	.015
Right hemisphere				
Middle temporal gyrus	ns	ns	.214	.049
Superior & transverse occipital sulcus	.349	.001	−.271	.012
Superior segment of the circular insular sulcus	.394	<.001	−.248	.022
Inferior part of the precentral sulcus	.251	.021	ns	ns
Medial occipito-temporal (lingual) sulcus	.255	.019	ns	ns
Parieto-occipital sulcus	.277	.010	ns	ns
Superior temporal sulcus	.226	.038	ns	ns
Suborbital sulcus	ns	ns	−.277	.010

Investigating the relationship between select subject variables and mean cortical curvature revealed a significant positive correlation between age of first mTBI injury and mean curvature in the left hemisphere middle occipital gyrus, left superior and transverse occipital sulcus, left orbital sulcus, right hemisphere intermedius primus of Jensen sulcus, and right superior and transverse occipital sulcus (see Table 4 and Fig. 5). After controlling for the effects of age of first injury, the time since the most recent mTBI was positively correlated with mean cortical curvature in the left inferior temporal sulcus, right superior frontal gyrus, and right superior frontal sulcus.

4. Discussion

As hypothesized, extensive regions of the cortex were identified that exhibited significantly increased mean cortical curvature at the gray–white matter junction in a sample of veterans with mTBI compared to controls. These differences were more prominent in sulcal regions of the cortex as opposed to gyral regions. Furthermore, gray and white matter volumes were differentially associated with increasing mean cortical curvature in gyral and sulcal regions. These findings suggest that alterations to cytoarchitecture during the chronic phase of mTBI can be assessed using measures of mean cortical curvature via regionally specific increases. Further, these findings support the idea that unique patterns of gray and white matter atrophy vary across the cortex and deeper regions of the cortex may be more adversely affected by mTBI.

4.1. Similarities to and departures from prior literature

The current study found increased mean cortical curvature in both sulcal and gyral regions that were related to changes in white and gray matter volumes in mTBI and is the first study to assess the relationship between mean cortical curvature and TBI compared to controls. However, Irimia et al. (2012) included mean cortical curvature as one of five representative statistics used to create patient-tailored connectomics geared toward assessing white matter atrophy. While their design was detailed 3 male adults with mild to severe TBI, many of the regions they identified as having been impacted by TBI are shared with the population of this study including the angular gyrus, Jensen's sulcus, superior temporal sulcus, and supramarginal gyrus. Similar to Irimia et al., the current study tested for effects across multiple regions of the cortex. Due to the heterogeneous nature inherent in TBI cohorts and the difficulties in detecting diminutive changes related to more mild injuries, it may prove valuable to explore several distinct regions of the cortex in addition to subcortical and whole brain analyses. For example, Zhou et al. (2013) conducted a longitudinal analysis on 28 subjects with TBI that assessed gyral and sulcal cortical gray matter, whole brain, subcortical, and white matter volumes near the time of injury and again approximately one-year post-injury. Regions indicating a significant difference in the longitudinal analysis were also compared to a sample of 22 controls in a cross-sectional analysis. The longitudinal analysis revealed significant white matter volume loss in regionally specific regions including bilateral anterior cingulate white matter volumes, left cingulate gyrus isthmus white matter, right inferior and medial orbital olfactory gray matter volumes, and right precuneus volume. All regions identified at the one-year follow up except the right inferior gray matter volume were also significantly reduced in TBI compared to controls.

Warner et al. (2010) also assessed longitudinal changes in global and regional brain volumes. Their study included 25 subjects with diffuse traumatic axonal injury and 22 age- and sex-matched controls. When comparing initial and follow-up scans, they found substantial global atrophy, decreased volume in many subcortical gray matter regions, and atrophy in 13 cortical regions out of 62 assessed. Reporting on the wide range neuroimaging results related to TBI that support global and regionally specific atrophy in TBI is outside the scope of this report; however, a recent review by Bigler (Bigler, 2013a) presents a comprehensive summary. Briefly, TBI frequently results in cerebral atrophy often impacting frontotemporolimbic regions. Injuries are often more disruptive to white matter neural connectivity. Additionally, TBI may demonstrate degenerative effects over time, which could predispose individuals to the development of other neurodegenerative and neuropsychiatric disorders (Bigler, 2013b).

4.2. Mean cortical curvature is an effective measurement of change

As previously mentioned, this study is the first to focus on how mTBI impacts mean cortical curvature compared to controls. However, mean cortical curvature has been used as a metric of change in a number of other study populations. For example, previous work conducted by Magnotta et al. (1999) suggested a model of atrophy associated with aging that includes increasing curvature in gyral regions and decreasing curvature in sulcal regions. They suggest that this pattern may best reflect age associated atrophic changes. While their model may appear to be in conflict with the current study's hypothesis of increased

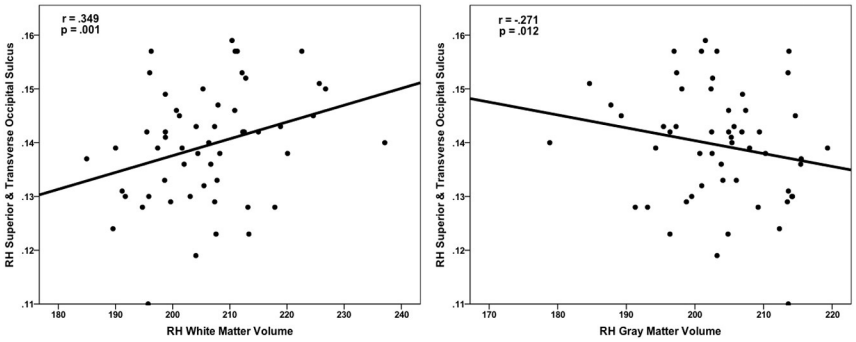

Fig. 4. Correlations between mean cortical curvature and white and gray matter volumes adjusted for total brain volume.

Table 4
Correlations between measures of select subject variables and mean cortical curvature.

	r	p
Age at first injury after the age of 12 (years)		
LH middle occipital gyrus	.324	.017
LH superior & transverse occipital sulcus	.448	.001
LH orbital sulcus	.283	.038
RH intermedius primus (of Jensen) sulcus	.277	.042
RH superior & transverse occipital sulcus	.268	.050
Time since most recent mTBI (months)[a]		
LH inferior temporal sulcus	.303	.029
RH superior frontal gyrus	.305	.028
RH superior frontal sulcus	.356	.009

[a] Adjusted for age at first injury after the age of 12.

curvature in sulcal regions, it is important to note that the main findings in the study by Magnotta et al. included curvature values averaged across all sulcal and gyral regions and were measured in healthy controls. The current study assessed curvature in distinct cortical regions. Furthermore, it has been suggested that brain volume loss associated with normal aging can be accelerated in instances of TBI (Bigler, 2013b). Findings from this investigation demonstrate a positive relationship between the time since the most recent TBI and mean cortical curvature as well as a positive relationship between subject age at the time of first injury and mean cortical curvature. These findings may point to an accelerated rate at which cortical curvature values increase over time due to injury.

Mean cortical curvature has also been investigated in psychiatric populations. For instance, White et al. (2003) found significantly increased curvature in gyral regions and flattened curvature in sulcal regions in patients with childhood- and adolescent-onset schizophrenia compared to healthy controls. Curvature was also used to assess sulcal morphology changes related to cortical thickness and gyral white matter volume in mild cognitive impairment and Alzheimer's disease (Im et al., 2008). Their study found lower average mean curvature in sulcal regions that was associated with disease progression from controls to mild cognitive impairment to Alzheimer's disease. This change in sulcal shape was also associated with decreases in cortical thickness and gyral white matter volume. Studies investigating the effects of neurological disorders have also turned to cortical curvature to assess atrophy. Deppe et al. (2014) investigated the relationship between whole-brain surface-averaged rectified cortical extrinsic curvature, white matter volumes, and surface area in patients with multiple sclerosis, Alzheimer's disease, clinically isolated syndrome, and healthy controls. They hypothesized that increases in mean curvature would be associated with white matter volume decreases while surface area would remain unchanged. They found increased curvature was highly correlated with reduction in white matter volumes in the clinically isolated and multiple sclerosis groups while no systemic curvature increases were observed in the Alzheimer's group.

4.3. Cytoarchitecture adaptation involves gray and white matter restructuring

Increases in mean cortical curvature located at the gray–white matter boundary could be attributed to volume loss associated with underlying neuronal death and reduced white matter integrity. Alone, increases in mean cortical curvature values may not be enough to support this idea. However, data from the current study provide evidence that restructuring of cytoarchitecture may be taking place during the chronic period of mTBI. For example, increasing white matter volume in sulcal regions was associated with increasing mean cortical curvature. This could indicate a sharpening of the sulcus due in part to the reorganization of white matter into areas normally occupied by gray matter. This idea of sulcal sharpening is further supported by negative correlations found in some of the same sulcal regions where increasing curvature was associated with decreasing gray matter volumes. The relationships between gray and white matter volumes and mean cortical curvature were reversed in gyral regions. However, only two regions demonstrated significant correlations leaving a question as to whether gyral sharpening may be due solely to white matter atrophy. Nonetheless, due to the diffuse nature of the increases in mean cortical curvature in gyral regions found in this study, it is conceivable that white matter atrophy is also involved.

4.4. Limitations

Some of the more challenging difficulties associated with interpreting TBI research include the presence of premorbid conditions, the heterogeneous nature of the injury, and functional outcomes. In the current study sample, limited self-report information is available regarding the acute symptoms of mTBI and diagnoses were not verified by chart review. However many individuals reported they did not seek medical care at the time of the incident. Reliance on self-report of events that may have been impacted by the injury itself is problematic, nevertheless documentation of traumatic events by chart reviews in veterans can also prove challenging as many traumatic events may go unreported (Buck, 2011). Many subjects reported blast related injuries; however, no detailed information was available regarding the direction of, force of, or distance from the blast. It is noteworthy, therefore, that in the current study sample increased mean cortical curvature was found to be widespread throughout the cortex. This study found a relationship between two injury related variables and mean cortical curvature. Future studies should include additional metrics of injury severity to be investigated for possible relationships to mean cortical curvature variances. Furthermore, it has been demonstrated that a number of psychiatric disorders may impact mean cortical curvature and/or brain volumes (Im et al., 2008; van Tol et al., 2010; Ronan et al., 2011, 2012; Lopez-Larson et al., 2012). No significant mean cortical curvature differences were found in the mTBI group between veterans with and without any or all psychiatric comorbidities

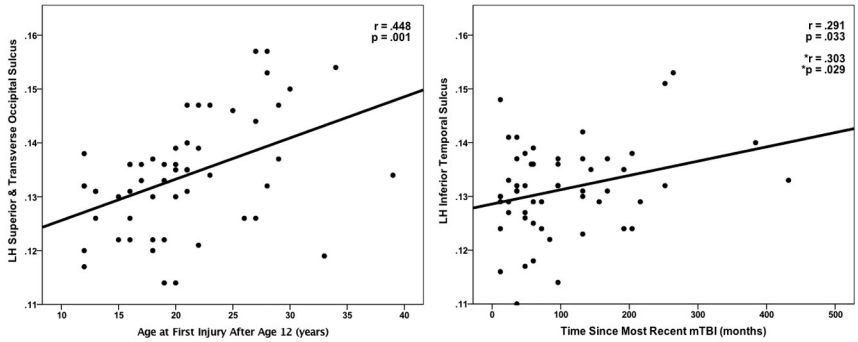

Fig. 5. Correlations between mean cortical curvature and select subject variables (*adjusted for age at first injury).

(mild depressive disorder, posttraumatic stress disorder, or substance use disorder). Despite this, these variables might impact the measures in ways not identified in the current study. Finally, as this study was structured using a cross-sectional design, caution needs to be used when interpreting results, as this type of study structure may include possible confounding factors not included in analysis. Future studies investigating the relationship between mean cortical curvature in TBI cohorts should incorporate a longitudinal design.

5. Conclusions

This study found widespread significant increases in mean cortical curvature in a sample of veterans with mTBI relative to controls. These differences were most prominent in deep gray matter regions of the cortex. Additionally, positive correlations were observed between cortical white matter volumes in sulcal regions whereas negative correlations were found between gray matter volumes in some of the same sulcal regions. Converse relationships between mean cortical curvature and gray and white matter volumes were found in gyral regions. These findings suggest potentially unique patterns of atrophy by region and indicate that changes in brain microstructure due to mTBI are sensitive to measures of mean curvature.

Acknowledgments

This work was supported by the Department of Veterans Affairs Salt Lake City Mental Illness Research, Education & Clinical Center (MIRECC), Merit Review 5I01CX000253-02 (PI Yurgelun-Todd). The authors would like to thank Elliott Bueler, Margaret Legaretta, PhD, and Erin McGlade, PhD for their contributions to this work including, but not limited to, subject recruitment and study management. We would also like to thank Jeffrey S. Anderson, MD, PhD for his feedback and assistance with methods, proof reading, and editing and Kagan R. Breitenbach for his assistance in figure creation.

Disclaimer: this article is based on work supported, in part, by the Department of Veterans Affairs, but does not necessarily represent the views of the Department of Veterans Affairs or the United States government.

References

American Psychiatric Association, 2000. Global assessment of functioning. Diagnostic and Statistical Manual of Mental Disorders: DSM-IV-TR, p. 32 (Washington, D.C.).

Amyot, F., Arciniegas, D.B., Brazaitis, M.P., Curley, K.C., Diaz-Arrastia, R., Gandjbakhche, A., Herscovitch, P., Hinds 2nd, S.R., Manley, G.T., Pacifico, A., Razumovsky, A., Riley, J., Salzer, W., Shih, R., Smirniotopoulos, J.G., Stocker, D., 2015. A review of the effectiveness of neuroimaging modalities for the detection of traumatic brain injury. J. Neurotrauma 32, 1693–1721.

Belanger, H.G., Uomoto, J.M., Vanderploeg, R.D., 2009. The Veterans Health Administration's (VHA's) Polytrauma System of Care for mild traumatic brain injury: costs, benefits, and controversies. J. Head Trauma Rehabil. 24, 4–13.

Benjamini, Y., Hochberg, Y., 1995. Controlling the false discovery rate: a practical and powerful approach to multiple testing. J. R. Stat. Soc. Ser. B Methodol. 57, 289–300.

Bigler, E.D., 2001. Distinguished Neuropsychologist Award Lecture 1999. The lesion(s) in traumatic brain injury: implications for clinical neuropsychology. Arch. Clin. Neuropsychol. 16, 95–131.

Bigler, E.D., 2013a. Neuroimaging biomarkers in mild traumatic brain injury (mTBI). Neuropsychol. Rev. 23, 169–209.

Bigler, E.D., 2013b. Traumatic brain injury, neuroimaging, and neurodegeneration. Front. Hum. Neurosci. 7, 395.

Bigler, E.D., Abildskov, T.J., Wilde, E.A., McCauley, S.R., Li, X., Merkley, T.L., Fearing, M.A., Newsome, M.R., Scheibel, R.S., Hunter, J.V., Chu, Z., Levin, H.S., 2010. Diffuse damage in pediatric traumatic brain injury: a comparison of automated versus operator-controlled quantification methods. Neuroimage 50, 1017–1026.

Buck, P.W., 2011. Mild traumatic brain injury: a silent epidemic in our practices. Health Soc. Work 36, 299–302.

Centers for Disease Control and Prevention, 2014. Report to Congress on Traumatic Brain Injury in the United States: Epidemiology and Rehabilitation. National Center for Injury Prevention and Control; Division of Unintentional Injury Prevention, Atlanta, GA.

Cole, J.H., Leech, R., Sharp, D.J., Alzheimer's Disease Neuroimaging I, 2015. Prediction of brain age suggests accelerated atrophy after traumatic brain injury. Ann. Neurol. 77, 571–581.

Coronado, V.G., McGuire, L.C., Sarmiento, K., Bell, J., Lionbarger, M.R., Jones, C.D., Geller, A.I., Khoury, N., Xu, L., 2012. Trends in traumatic brain injury in the U.S. and the public health response: 1995–2009. J. Saf. Res. 43, 299–307.

Corrigan, J.D., Bogner, J., 2007. Initial reliability and validity of the Ohio State University TBI Identification Method. J. Head Trauma Rehabil. 22, 318–329.

Dale, A.M., Sereno, M.I., 1993. Improved localization of cortical activity by combining EEG, and MEG with MRI cortical surface reconstruction: a linear approach. J. Cogn. Neurosci. 5, 162–176.

Dale, A.M., Fischl, B., Sereno, M.I., 1999. Cortical surface-based analysis. I. Segmentation and surface reconstruction. Neuroimage 9, 179–194.

Deppe, M., Marinell, J., Kramer, J., Duning, T., Ruck, T., Simon, O.J., Zipp, F., Wiendl, H., Meuth, S.G., 2014. Increased cortical curvature reflects white matter atrophy in individual patients with early multiple sclerosis. Neuroimage Clin. 6, 475–487.

Desikan, R.S., Segonne, F., Fischl, B., Quinn, B.T., Dickerson, B.C., Blacker, D., Buckner, R.L., Dale, A.M., Maguire, R.P., Hyman, B.T., Albert, M.S., Killiany, R.J., 2006. An automated labeling system for subdividing the human cerebral cortex on MRI scans into gyral based regions of interest. Neuroimage 31, 968–980.

Destrieux, C., Fischl, B., Dale, A., Halgren, E., 2010. Automatic parcellation of human cortical gyri and sulci using standard anatomical nomenclature. Neuroimage 53, 1–15.

Ding, K., Marquez de la Plata, C., Wang, J.Y., Mumphrey, M., Moore, C., Harper, C., Madden, C.J., McColl, R., Whittemore, A., Devous, M.D., Diaz-Arrastia, R., 2008. Cerebral atrophy after traumatic white matter injury: correlation with acute neuroimaging and outcome. J. Neurotrauma 25, 1433–1440.

First, M., Spitzer, R., Gibbon, M., Williams, J., 1996. Structured Clinical Interview for the DSM-IV Axis I Disorders.

Fischl, B., Dale, A.M., 2000. Measuring the thickness of the human cerebral cortex from magnetic resonance images. Proc. Natl. Acad. Sci. U. S. A. 97, 11050–11055.

Fischl, B., Liu, A., Dale, A.M., 2001. Automated manifold surgery: constructing geometrically accurate and topologically correct models of the human cerebral cortex. IEEE Trans. Med. Imaging 20, 70–80.

Fischl, B., Salat, D.H., Busa, E., Albert, M., Dieterich, M., Haselgrove, C., van der Kouwe, A., Killiany, R., Kennedy, D., Klaveness, S., Montillo, A., Makris, N., Rosen, B., Dale, A.M., 2002. Whole brain segmentation: automated labeling of neuroanatomical structures in the human brain. Neuron 33, 341–355.

Fischl, B., Salat, D.H., van der Kouwe, A.J., Makris, N., Segonne, F., Quinn, B.T., Dale, A.M., 2004a. Sequence-independent segmentation of magnetic resonance images. Neuroimage 23 (Suppl. 1), S69–S84.

Fischl, B., van der Kouwe, A., Destrieux, C., Halgren, E., Segonne, F., Salat, D.H., Busa, E., Seidman, L.J., Goldstein, J., Kennedy, D., Caviness, V., Makris, N., Rosen, B., Dale, A.M., 2004b. Automatically parcellating the human cerebral cortex. Cereb. Cortex 14, 11–22.

Guadalupe, T., Zwiers, M.P., Wittfeld, K., Teumer, A., Vasquez, A.A., Hoogman, M., Hagoort, P., Fernandez, G., Buitelaar, J., van Bokhoven, H., Hegenscheid, K., Völzke, H., Franke, B., Fisher, S.E., Grabe, H.J., Francks, C., 2015. Asymmetry within and around the human planum temporale is sexually dimorphic and influenced by genes involved in steroid hormone receptor activity. Cortex 62, 41–55.

Han, K., Mac Donald, C.L., Johnson, A.M., Barnes, Y., Wierzechowski, L., Zonies, D., Oh, J., Flaherty, S., Fang, R., Raichle, M.E., Brody, D.L., 2014. Disrupted modular organization of resting-state cortical functional connectivity in U.S. military personnel following concussive 'mild' blast-related traumatic brain injury. Neuroimage 84, 76–96.

Huang, M.X., Theilmann, R.J., Robb, A., Angeles, A., Nichols, S., Drake, A., D'Andrea, J., Levy, M., Holland, M., Song, T., Ge, S., Hwang, E., Yoo, K., Cui, L., Baker, D.G., Trauner, D., Coimbra, R., Lee, R.R., 2009. Integrated imaging approach with MEG and DTI to detect mild traumatic brain injury in military and civilian patients. J. Neurotrauma 26, 1213–1226.

Im, K., Lee, J.M., Seo, S.W., Hyung Kim, S., Kim, S.I., Na, D.L., 2008. Sulcal morphology changes and their relationship with cortical thickness and gyral white matter volume in mild cognitive impairment and Alzheimer's disease. Neuroimage 43, 103–113.

Iraji, A., Chen, H., Wiseman, N., Haacke, E.M., Liu, T., Kou, Z., 2016. Compensation through functional hyperconnectivity: a longitudinal connectome assessment of mild traumatic brain injury. Neural Plast. 2016, 13, 4072402. http://dx.doi.org/10.1155/2016/4072402.

Irimia, A., Chambers, M.C., Torgerson, C.M., Filippou, M., Hovda, D.A., Alger, J.R., Gerig, G., Toga, A.W., Vespa, P.M., Kikinis, R., Van Horn, J.D., 2012. Patient-tailored connectomics visualization for the assessment of white matter atrophy in traumatic brain injury. Front. Neurol. 3, 10.

Irimia, A., Goh, S.Y., Torgerson, C.M., Vespa, P., Van Horn, J.D., 2014. Structural and connectomic neuroimaging for the personalized study of longitudinal alterations in cortical shape, thickness and connectivity after traumatic brain injury. J. Neurosurg. Sci. 58, 129–144.

Lopez-Larson, M.P., King, J.B., Terry, J., McGlade, E.C., Yurgelun-Todd, D., 2012. Reduced insular volume in attention deficit hyperactivity disorder. Psychiatry Res. 204, 32–39.

Lopez-Larson, M., King, J.B., McGlade, E., Bueler, E., Stoeckel, A., Epstein, D.J., Yurgelun-Todd, D., 2013. Enlarged thalamic volumes and increased fractional anisotropy in the thalamic radiations in veterans with suicide behaviors. Front. Psychiatry 4, 83.

Luders, E., Thompson, P.M., Narr, K.L., Toga, A.W., Jancke, L., Gaser, C., 2006. A curvature-based approach to estimate local gyrification on the cortical surface. Neuroimage 29, 1224–1230.

Magnotta, V.A., Andreasen, N.C., Schultz, S.K., Harris, G., Cizadlo, T., Heckel, D., Nopoulos, P., Flaum, M., 1999. Quantitative in vivo measurement of gyrification in the human brain: changes associated with aging. Cereb. Cortex 9, 151–160.

Maudsley, A.A., Govind, V., Levin, B., Saigal, G., Harris, L., Sheriff, S., 2015. Distributions of magnetic resonance diffusion and spectroscopy measures with traumatic brain injury. J. Neurotrauma 32, 1056–1063.

Mayer, A.R., Bellgowan, P.S., Hanlon, F.M., 2015. Functional magnetic resonance imaging of mild traumatic brain injury. Neurosci. Biobehav. Rev. 49, 8–18.

Operto, G., Auzias, G., Le Troter, A., Perrot, M., Riviere, D., Dubois, J., Huppi, P., Coulon, O., Mang, J., 2012. Structural group analysis of cortical curvature and depth patterns in the developing brain. Biomedical Imaging (ISBI), 2012 9th IEEE International Symposium on, pp. 422–425.

Osborn, A.G., 2010. Diagnostic Imaging. Amirsys, Salt Lake City, Utah.

Palacios, E.M., Sala-Llonch, R., Junque, C., Roig, T., Tormos, J.M., Bargallo, N., Vendrell, P., 2013. White matter/gray matter contrast changes in chronic and diffuse traumatic brain injury. J. Neurotrauma 30, 1991–1994.

Petrie, E.C., Cross, D.J., Yarnykh, V.L., Richards, T., Martin, N.M., Pagulayan, K., Hoff, D., Hart, K., Mayer, C., Tarabochia, M., Raskind, M.A., Minoshima, S., Peskind, E.R., 2014. Neuroimaging, behavioral, and psychological sequelae of repetitive combined blast/impact mild traumatic brain injury in Iraq and Afghanistan war veterans. J. Neurotrauma 31, 425–436.

Pienaar, R., Fischl, B., Caviness, V., Makris, N., Grant, P.E., 2008. A methodology for analyzing curvature in the developing brain from preterm to adult. Int. J. Imaging Syst. Technol. 18, 42–68.

Ronan, L., Scanlon, C., Murphy, K., Maguire, S., Delanty, N., Doherty, C.P., Fitzsimons, M., 2011. Cortical curvature analysis in MRI-negative temporal lobe epilepsy: a surrogate marker for malformations of cortical development. Epilepsia 52, 28–34.

Ronan, L., Voets, N.L., Hough, M., Mackay, C., Roberts, N., Suckling, J., Bullmore, E., James, A., Fletcher, P.C., 2012. Consistency and interpretation of changes in millimeter-scale cortical intrinsic curvature across three independent datasets in schizophrenia. Neuroimage 63, 611–621.

Schaer, M., Cuadra, M.B., Tamarit, L., Lazeyras, F., Eliez, S., Thiran, J.P., 2008. A surface-based approach to quantify local cortical gyrification. IEEE Trans. Med. Imaging 27, 161–170.

Segonne, F., Dale, A.M., Busa, E., Glessner, M., Salat, D., Hahn, H.K., Fischl, B., 2004. A hybrid approach to the skull stripping problem in MRI. Neuroimage 22, 1060–1075.

Segonne, F., Pacheco, J., Fischl, B., 2007. Geometrically accurate topology-correction of cortical surfaces using nonseparating loops. IEEE Trans. Med. Imaging 26, 518–529.

Shenton, M.E., Hamoda, H.M., Schneiderman, J.S., Bouix, S., Pasternak, O., Rathi, Y., Vu, M.A., Purohit, M.P., Helmer, K., Koerte, I., Lin, A.P., Westin, C.F., Kikinis, R., Kubicki, M., Stern, R.A., Zafonte, R., 2012. A review of magnetic resonance imaging and diffusion tensor imaging findings in mild traumatic brain injury. Brain Imaging Behav. 6, 137–192.

Sled, J.G., Zijdenbos, A.P., Evans, A.C., 1998. A nonparametric method for automatic correction of intensity nonuniformity in MRI data. IEEE Trans. Med. Imaging 17, 87–97.

Smith, D.H., Johnson, V.E., Stewart, W., 2013. Chronic neuropathologies of single and repetitive TBI: substrates of dementia? Nat. Rev. Neurol. 9, 211–221.

Trivedi, M.A., Ward, M.A., Hess, T.M., Gale, S.D., Dempsey, R.J., Rowley, H.A., Johnson, S.C., 2007. Longitudinal changes in global brain volume between 79 and 409 days after traumatic brain injury: relationship with duration of coma. J. Neurotrauma 24, 766–771.

van Tol, M.J., van der Wee, N.J., van den Heuvel, O.A., Nielen, M.M., Demenescu, L.R., Aleman, A., Renken, R., van Buchem, M.A., Zitman, F.G., Veltman, D.J., 2010. Regional brain volume in depression and anxiety disorders. Arch. Gen. Psychiatry 67, 1002–1011.

Wang, J., Li, W., Miao, W., Dai, D., Hua, J., He, H., 2014. Age estimation using cortical surface pattern combining thickness with curvatures. Med. Biol. Eng. Comput. 52, 331–341.

Warner, M.A., Youn, T.S., Davis, T., Chandra, A., Marquez de la Plata, C., Moore, C., Harper, C., Madden, C.J., Spence, J., McColl, R., Devous, M., King, R.D., Diaz-Arrastia, R., 2010. Regionally selective atrophy after traumatic axonal injury. Arch. Neurol. 67, 1336–1344.

White, T., Andreasen, N.C., Nopoulos, P., Magnotta, V., 2003. Gyrification abnormalities in childhood- and adolescent-onset schizophrenia. Biol. Psychiatry 54, 418–426.

Yurgelun-Todd, D.A., Bueler, C.E., McGlade, E.C., Churchwell, J.C., Brenner, L.A., Lopez-Larson, M.P., 2011. Neuroimaging correlates of traumatic brain injury and suicidal behavior. J. Head Trauma Rehabil. 26, 276–289.

Zhou, Y., Kierans, A., Kenul, D., Ge, Y., Rath, J., Reaume, J., Grossman, R.I., Lui, Y.W., 2013. Mild traumatic brain injury: longitudinal regional brain volume changes. Radiology 267, 880–890.